Surface Pressure Measurements in Shock Wave/Boundary-Layer Interactions

Yeol Lee*, Sanjay Garg and Gary S. Settles*****

(Received November 20, 1995)

An experimental research program establishing a database of the surface pressure in swept shock wave/boundary-layer interactions is described. An equilibrium turbulent boundary-layer on a flat plate is subjected to impingement by swept planar shock waves genterated by a sharp fin. Various fin angles at 4 different freestream Mach numbers produce a variety of interaction strengths from weak to very strong. For each of different interaction cases, the surface flow patterns are obtained by a kerosene-lampblack-adhesive transparent tape technique. Surface pressures within the interactions are also measured from several streamwise row of taps connected to a computer-controlled Scanivalve system. An extensive error analysis is carried out for the experiments yielding an uncertainty of about $\pm 3\%$. From these measurements, high spatial resolution surface pressure distributions for different interaction cases are obtained.

Key Words: Pressure Measurements, Shock Wave, Boundary-Layer Interactions, Separation, λ-Shock Structure

Nomenclature

M	: Mach number
p	: Surface static pressure
R	: Radial distance from fin leading-edge
VCO	: Virtual conical origin
α	: Angle-of-attack of the fin
β	: Angle with respect to incoming free-stream direction, measured from fin leading-edge

Subscripts

pa	: Primary attachment
peak	: Peak value
ps	: Primary separation
ss	: Secondary separation
ui	: Upstream influence
∞	: Incoming freestream
n	: Normal component

* Assistant Professor, Department of Aeronautical & Mechanical Engineering, Hankuk Aviation University, Korea.

** Research Scientist, High Technology Corporation, Hampton, VA 23666, U.S.A.

*** Professor, Department of Mechanical Engineering, Pennsylvania State University, University Park, PA 16802, U.S.A.

1. Introduction

The study of shock wave/turbulent boundary-layer interactions is important to the solution of internal and external aerodynamic/aerothermal problems in the design of high-speed vehicles, as well as for the validation of the associated numerical simulations.

When an oblique shock wave of sufficient strength impinges upon a solid surface and interacts with the turbulent boundary-layer on that surface, a three-dimensional separated region is generated there. Peak values of surface pressure, skin friction and heat transfer are then observed to occur near the attachment-line of this separated flow. These peak values are of great practical importance in establishing the limits of mean aerodynamic and aerothermal loads on high-speed flight vehicles. Accurate experimental measurements of pressure, skin friction and heat transfer distributions in the interactions are therefore important for this purpose.

The salient feature of the swept-sharp fin inter-

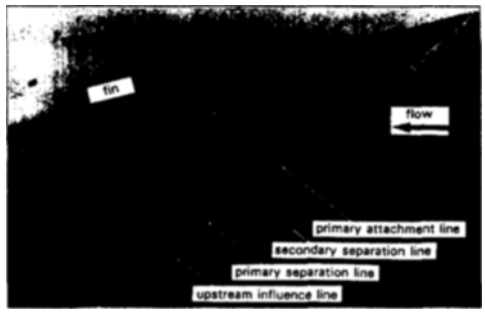

Fig. 1 Surface streamline pattern ($M_\infty=3.0$, $\alpha=20°$)

action is its quasi-conical symmetry. This has been observed by many investigators and recently confirmed by parametric studies (Lu and Settles, 1983; Alvi and Settles, 1991). The interaction growth is essentially conical except for an initial region in the immediate vicinity of the juncture of the fin-leading-edge and the flat plate. The topological features of the interaction flow appear to emanate from a single point, which has been termed the "Virtual Conical Origin" (VCO). According to Lu and Settles(1983), the curved, non-conical region near the VCO is called the "inception zone." Beyond this zone, all limiting streamline patterns show conical symmetry characteristics. To demonstrate these characteristics, Fig. 1 shows an example of the suface streamline pattern obtained by the kerosene-lampblack technique for an interaction of $M_\infty=3.0$ and the fin-angle-of attack $\alpha=16°$.

Not only the surface features, but also the flowfield structure above the surface of these swept interactions show quasiconical behavior. Oskam *et al.* (1975) was among the first investigators to study the flowfield structure of sharp-fin-generated swept interactions. Zubin and Ostapenko (1979) also provided discussions of the conical characteristics of sharp fin interactions. They found that the interaction was purely conical, except for an inception zone near the leading-edge of the fin. Finally from experiments using the conical shadowgraph technique and the PLS (Planar Laser Scattering) technique, Alvi and Settles (1990, 1991) have produced a comprehensive physical model of the flowfield structure

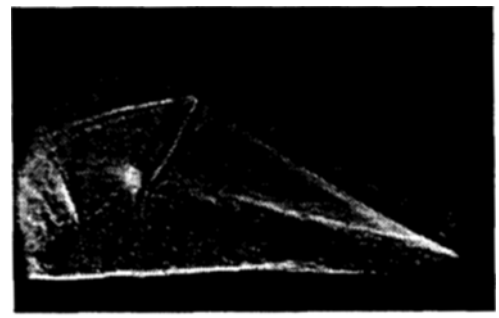

(a)

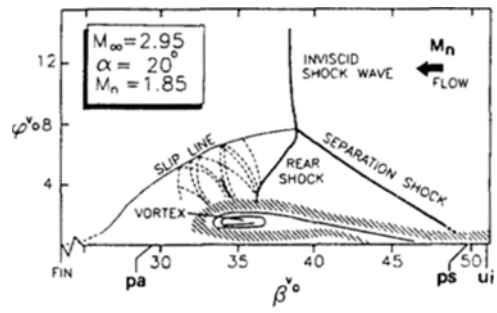

(b)

Fig. 2 Conical flowfield structure

and the behavior of fin-generated swept interactions, which has been constructed in spherical polar coordinates.

Figure 2(a) shows a shadowgram image for $M_\infty=3.0$, $\alpha=20°$, as an illustration of the conical interaction flowfield. Their flowfield model is also shown in Fig. 2(b) for comparison. Figure 2 (b) is shown in conical ϕ, β angular coordinates, where the superscript v_o denotes the measurement with respect to the VCO (for the conical ϕ, β coordinates, see Fig. 3). By taking advantage of this conical symmetry behavior, the normal Mach number, M_n, can be used as an interaction strength panameter to first order. The normal Mach number, M_n, is defined as the normal component of the freestream Mach number with respect to the inviscid shock wave.

Most recently, new data have been obtained on the structure of these interactions from the parametric studies of the Penn State University Gas Dynamics Laboratory. Kim *et al.* (1991) mea-

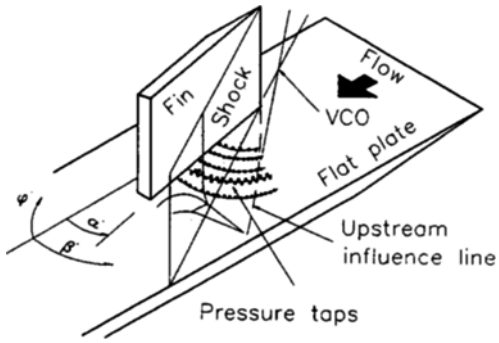

Fig. 3 Sketch of test geometry.

sured the distrλbution of skin friction in the interactions using the laser interferometer skin friction (LISF) meter. Also Lee *et al.* (1994) measured the distribution of heat transfer using the Resistance Heater Method in the same interactions. Reviews by Settles and Dolling (1986, 1990) cover the progress of research on the swept interaction problem.

In addition to the time-averaged behavior of the interactions, turbulence and unsteady shock motion result in fluctuation of pressure, skin friction and heat transfer in such flows, which are sources of serious additional loads of an unsteady nature. Unsteady phenomena in shock boundary-layer interactions have mainly been studied via fluctuating surface pressure measurements. Gibson and Dolling (1991) measured wall pressure fluctuations in Mach 5 sharp-fin induced interactions and found that the unsteadiness had conical characteristics in general, following the mean flow trend. Garg and Settles (1993) made detailed measurements of unsteady surface pressure in Mach 3 and 4 sharp fin interactions. They found that the magintude of these pressure fluctuations was largest near the primary attachment line, and they explained that the cause of this peak in rms pressure was a random unsteady motion of the primary attachment line. Much of the information on unsteady phenomena in the shock/boundary-layer interactions has been reviewed by Dolling (1993).

The present work has been carried out to obtain new benchmark data of mean surface pressure in a variety of interaction strengths.

2. Experimental Methods

2.1 Wind tunnel facility and test conditions

The experiments were performed in the Penn State University Gas Dynamics Laboratory's supersonic wind tunnel facility, which is an intermittent blowdown tunnel with a test section size of $15cm \times 17cm \times 60cm$. The facility has a unique variable Mach number capability over the range of Mach 1.5 to 4.0 by way of an asymmetric sliding-block nozzle. A $57m^3$, 2.0 *Mpa* pressure reservior provides testing times up to 2 minutes at stagnation pressure up to 1.5 *Mpa* and a near-ambient stagnation temperature. The experiments described in this paper were performed from freestream Mach number 2.5 to 4.0, with corresponding mass flow rate of $11.2kg/s$ and $8.0kg/s$, respectively.

2.2 Fin and flat plate

The interaction is generated by an equilibrium, adiabatic flat plate boundary-layer interacting with the swept, planar oblique shock wave generated by an upright, sharp-leading-edge fin at an angle of attack (see Fig. 3). The fin leading edge is $21.6cm$ aft of the plate leading edge. The strength of the interactions is controlled by changing the angle of attack of the fin. The movement of the fin is controlled by a pneumatic fin-injection mechanism, which is mounted through the tunnel side wall. The flat plate contains 96 surface pressure taps which are laid out along 5 circular arcs centered at the fin leading edge (see Fig. 3). The radial distribution of the pressure taps is based on the concept of conical symmetry of the interactions, which has been discussed before. From the same viewpoint, only data from the 3rd and 4th circular arcs ($R=76mm$ and $R=101mm$) are used for final results of pressure distributions inside the interactions, while all data has been taken from the 96 pressure taps.

2.3 Turbulent boundary-layer without fin

The undisturbed boundary-layer on the flat plate without fin is 2-dimensional and turbulent. Natural boundary-layer transition on the plate

typically occurs within 1-2 cm of the flat-plate leading edge at the present high Reynolds numbers. Also the present turbulent boundary-layer on the flat plate is naturally in a near-adiabatic condition (the ratio of the wall temperature, T_w, to the adiabatic wall temperature, T_{aw}, is typically 1.03). For the tested 4 different freestream Mach numbers of 2.5, 3.0, 3.5 and 4.0, the characteristics of the undisturbed boundary-layer at a position 22.7cm downstream of the flat plate leading edge (which is close to the location of fin leading edge) is given in Table 1.

2.4 Instrumentation

Two Scanivalve channels are used for scanning the 96 pressure taps during the tunnel running time. The signal from the scanivalve pressure transducer is sampled at the rate of 2 kHz by a Metrabyte Dash-16 A/D board. Fifteen samples are averaged for each surface pressure. The total data acquisition time for scanning all pressure taps is about 22 seconds. During each scanivalve stop, a dwell time of about 0.3 seconds is allowed to elapse before taking the data. This dwell time was proven to be sufficiently long to allow the pressure in the connecting tubes to equilibrate.

A weak streamwise pressure gradient, which exists on the flat plate with no fin in place due to weak waves in the test section, can affect the characteristics of the present interactions. To check this, the surface pressure at 96 locations on the flat plate were measured without fin in place, and it is found that the standard deviation of these surface pressures is about 3% of the mean value. Therefore, it is believed the present streamwise pressure gradient on the flat plate is too weak to affect the interactions, and it was neglected in the present experiments.

Table 1 Undisturbed flat plate boundary-layer

M_∞	δ (mm)	δ^* (mm)	θ (mm)	Re/l ($/m$)
2.5	3.88	1.00	0.16	5.4E7
3.0	3.64	1.05	0.16	5.9E7
3.5	3.21	0.95	0.16	6.4E7
4.0	3.10	0.98	0.12	7.6E7

2.5 Error analysis

The uncertainty of each variable in the above process contributes to the total uncertainty of the final result. As Coleman and Steele (1989) have suggested, the total uncertainty of the present measurements is determined by calculating and combining the "root-sum-squares" of the uncertainties of each variable in the data reduction equation. The errors of the surface pressure measurement, due to electric noise, repeatability and pressure calibration uncertainties were carefully examined, and total uncertainties of the present measurements are estimated to be within the range of $\pm 3.0\%$. This accuracy level is believed to qualify the present results as "benchmark" data for code validation.

3. Results and Discussion

Various fin angles at 4 different freestream Mach numbers generates 32 different interaction strengths from weak to very strong. From Fig. 4 to Fig. 8, the surface pressure distribution normalized with respect to the freestream pressure, p/p_∞, in the five representative shock wave/boundary-layer interactions are plotted versus the angle β measured from the fin leading-edge. The angles of the surface limiting streamlines, which were measured by a surface flow visualization technique (kerosene-lampblack tracing), the location of the inviscid shock, and the pressure-jump

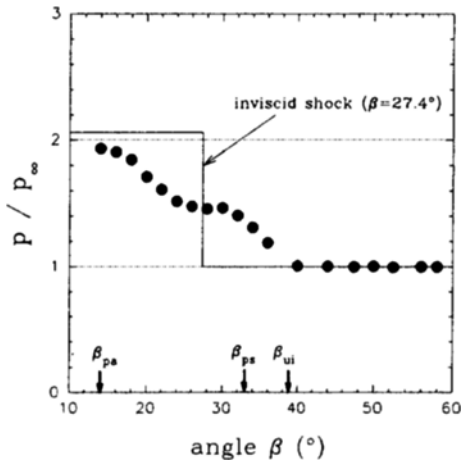

Fig. 4 p/p_∞ vs. β for $M_\infty=3.0$, $\alpha=10°$ ($M_n=1.4$).

across the inviscid shock wave determined by the normal shock table are also shown in these figures. Here, β_{pa}, β_{ss}, β_{ps}, and β_{ui} represent the angle of the primary attachment, secondary separation, primary separation and upstream influence, respectively. They are measured with respect to the fin-leading-edge.

For the $M_\infty=3.0$, $\alpha=10^\circ$ interaction (Fig. 4), little variation of pressure is observed outside the upstream influence line ($\beta_{ui}=39^\circ$) of the interaction. However, after the upstream influence line, a rise in the pressure occurs beneath the inviscid shock, reaching a maximum value of 1.9 times the incoming level at the attachment line, $\beta_{pa}=14^\circ$. A physical interpretation of this increase of surface pressure inside the interation is possible in terms of the "λ-shock" structure (see Fig. 2). The λ-shock causes the incoming boundary-layer to separate and this flow to turn and impinge upon the flat plate surface near the fin as a jet. The pressure of the flow is increased after the separation shock and the rear shock.

Therefore, it is postulated that the peak surface pressure occurring near the fin is due to the λ-shock structure and the process of attachment of the swept separated flow and the impinging-jet structure. This phenomenon is known to produce high surface pressure and high skin friction (Kim *et al.*, 1991) as well as high heat transfer levels (Lee *et al.*, 1994). Also, visualizations of such swept interactions by conical shadowgraphy (Alvi and Settles, 1990) show this jet impingement quite clearly.

The measured surface pressure distribution for the $M_\infty=3.0$, $\alpha=16^\circ$ interaction is shown in Fig. 5. This stronger interation exhibits the same qualitative features as the $\alpha=10^\circ$ case. Again, the level of pressure begins to increase through the location of the inviscid shock and the peak surface pressure occurs at $\beta=22^\circ$. This is where the primary attachment line is observed in surface flow visualizations ($\beta_{pa}=23^\circ$). The peak level now increases up to 3.1 times the incoming pressure level. As the interaction strength grows, the pressure jump across the λ-shock structure increases and the jet impingement strength also grows and produces higher local surface pressure.

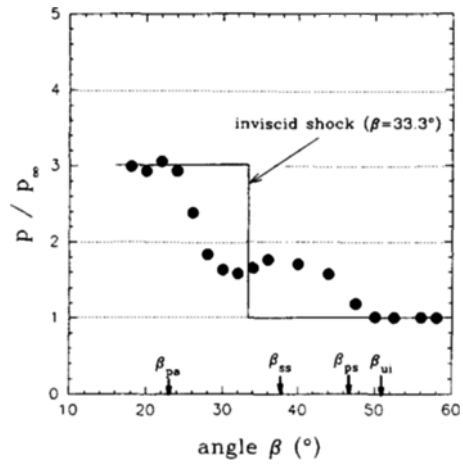

Fig. 5 p/p_∞ vs. β for $M_\infty=3.0$, $\alpha=16^\circ$ ($M_n=1.6$).

One interesting phenomenon observed in this interaction case is that a small local peak is observed near the secondary separation line ($\beta_{ss}=38^\circ$). This peak was not observed in the weaker $M_\infty=3.0$, $\alpha=10^\circ$ interaction, but for the present case the secondary separation line is evident in the surface-flow pattern. In surface flow patterns, the so-called secondary separation line appears as a discontinuity in the surface streamlines. The conical shadowgrams taken by Alvi and Settles (1991) show an obvious bulge in the reversed flow near that region. Also Zheltovodov *et al.* (1987) have observed distinct secondary separation for strong interactions.

In Fig. 6 the surface pressure distribution for the $M_\infty=3.0$, $\alpha=20^\circ$ interaction is shown. After the separation the pressure begins to increase immediately and a local peak is observed aft of the secondary separation line ($\beta_{ss}=45^\circ$). According to Kim *et al.* (1991), the skin friction distributions also show a small secondary peak near the region of secondary separation. Lee *et al.* (1994) have further demonstrated that an apparent local peak of heat transfer near this secondary separation region appears in the present $M_\infty=3.0$, $\alpha=20^\circ$ interaction.

After the secondary separation line in Fig. 6, there is a sharp increase in the measured pressure, reaching a maximum of about 4.0 times the incoming pressure level near the primary flow

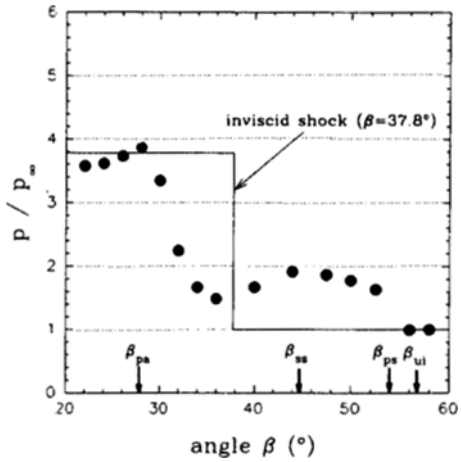

Fig. 6 p/p_∞ vs. β for $M_\infty=3.0$, $\alpha=20°$ ($M_n=1.9$).

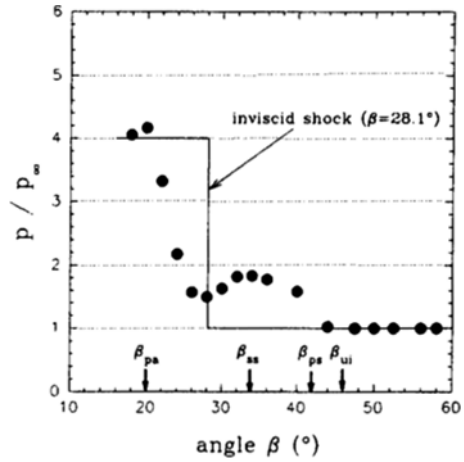

Fig. 7 p/p_∞ vs. β for $M_\infty=4.0$, $\alpha=16°$ ($M_n=1.9$).

attachment line ($\beta_{pa}=28°$). Again, this steep rise to the peak can be explained in terms of the pressure jump through the λ-shock structure and the impingement of the high-speed jet upon the flat plate in the vicinity of the primary attachment line. One interesting phenomenon in this interaction case is a decrease of the pressure near the fin after the primary attachment line. According to the present experiments including other interaction strengths, this pressure decrease after the primary attachment line appears in the range of $M_n=1.4\sim1.8$, is depending on the freestream Mach number.

In Fig. 7 the surface pressure distribution for the interaction case of $M_\infty=4.0$, $\alpha=16°$ is shown. After the separation line the pressure begins to increase up to the secondary separation line ($\beta_{ss}=34°$). The small local peak observed aft of the secondary separation line in the previous interaction is seen here also. A sharp increase in the pressure is again observed, reaching a maximum of about 4.2 times the incoming pressure level near the primary flow attachment line ($\beta_{pa}=20°$). This interaction and previous one ($M_\infty=3.0$, $\alpha=20°$) are expected to have some similarities, since they both have nearly the same normal Mach number M_n. Indeed the p_{peak}/p_∞ value is about 4 for both cases.

Finally, the surface pressure distribution for the strongest interaction, $M_\infty=4.0$, $\alpha=20°$ is shown in

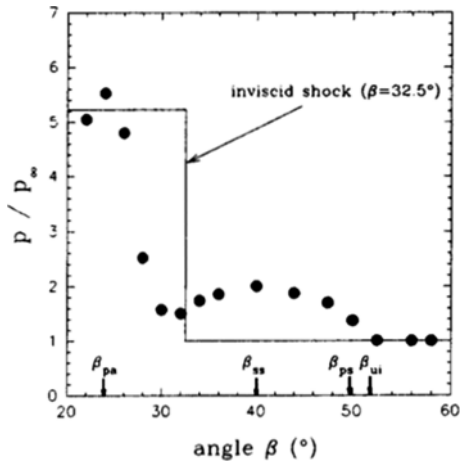

Fig. 8 p/p_∞ vs. β for $M_\infty=4.0$, $\alpha=20°$ ($M_n=2.1$).

Fig. 8. A comparison of the present experimental data for this case with numerical calculation can be found in Knight and Badekas's paper (1991). In Fig. 8, a local peak similar to that observed in the $M_\infty=3.0$, $\alpha=20°$ interaction is seen near the secondary separation line ($\beta_{ss}=40°$). After the primary separation line the pressure level increases sharply to a maximum of about 5.5 times the incoming pressure level near the primary flow attachment line ($\beta_{pa}=24°$). Especially for this very strong interaction case, the compression fan reflected from the slip line after the rear shock coalesces to form a "normal shock", which terminates supersonic flow in jet prior to its

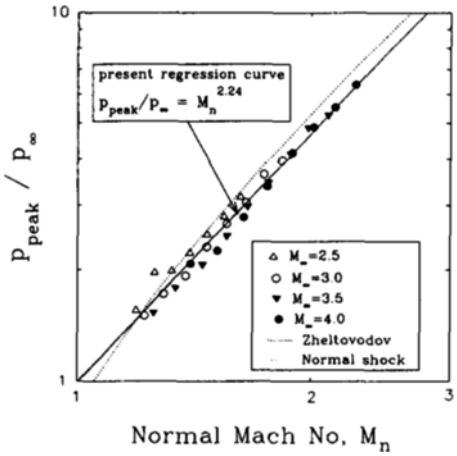

Fig. 9 Peak pressure correlation with M_n.

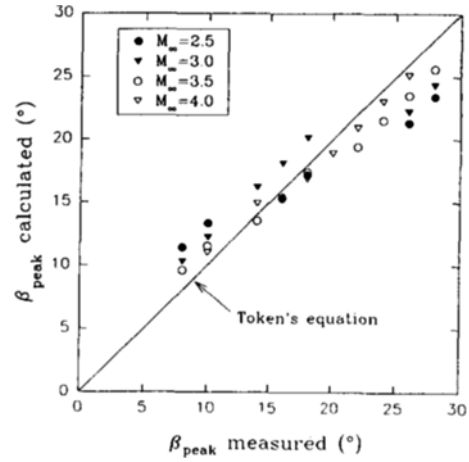

Fig. 10 Correlation of peak pressure location.

impingement and contributes to the highest surface pressure in the interaction.

Utilizing the quasiconical nature of the fin interaction, a simple correlation can be posed in terms of p_{peak}/p_∞ vs. M_n only. This correlation is demonstrated in Fig. 9. In the figure the present data are shown for 4 different freestream Mach numbers (32 data points). It is apparent that the all data points approximately describe a linear relationship (in log scale) with normal Mach number, M_n. For relatively weaker interaction cases (M_n less than about 1.6) a little scatter of the data points around the correlation curve is observed, which is postulated that the influence of the characteristics of freestream boundary-layer on the peak pressure is stronger for the weaker interactions. Consequently, different freestream Mach number has no strong influence upon the correlation curve. This agrees with the finding of Zubin and Ostapenko (1979) that the plateau pressure ratio in these interactions could be correlated purely as a function of M_n without regard to M_∞. Hayes' peak pressure function (1977) and pressure-jump determined by normal shock calculation are also shown in Fig. 9 for comparison. The equation of the regression line determined from the present experiments in Fig 9 is shown in the Eq. (1)

$$\frac{p_{peak}}{p_\infty} = M_n^{2.24} \tag{1}$$

This relationship is hereby proposed as a simple empirical guide for peak pressure in sharp-fin-generated interations with turbulent boundary-layers outboard of the inception zone near the fin leading edge.

Under the same consideration of the quasiconical nature of the fin interaction, the measured location of peak pressure is compared to Token's (1974) expression. Token (1974) proposed the correlation of the peak pressure location by:

$$\beta_{peak} = 0.24(\beta_{shock} - \alpha) \tag{2}$$

where β_{peak}, β_{shock} represent the angle of peak pressure and the angle of inviscid shock measured with respect to the fin leading edge, respectively. The present measured location of peak pressure is compared with Token's (1974) correlation equation in Fig. 10. Even though the uncertainty of the measured angle in present experiment ($\pm 2°$) is taken into account, there are apparent mismatch between the present experimental data and Token's expression. The reason is postulated due to taking the fin leading edge as the origin of the angle, rather than VCO. In other words a better correlation equation to experimental data could be obtained, if the origin of the angle is taken with respect to VCO. Unfortunately, the information of VCO for all present interation cases are not available at the present time.

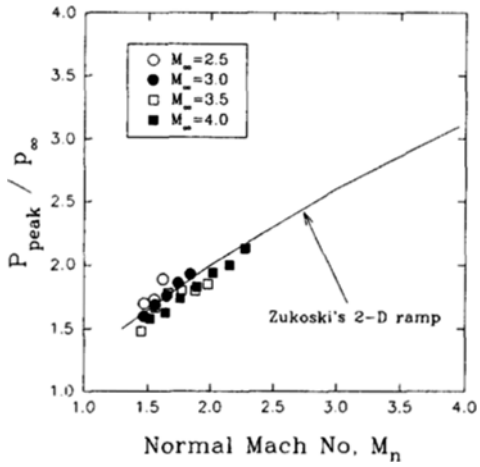

Fig. 11 Secondary peak pressure correlation with M_n.

Secondary separation which occur at moderate interaction strengths has also been one of prime interests. According to the present experiments the secondary separation begins to appear near $M_n=1.5$ regardless of freestream Mach number. By the same analogy as shown in Fig. 9, the pressure of the secondary peak inside the interaction can be correlated with the normal Mach number. In Fig. 11 the pressure of the secondary peak is correlated to the normal Mach number and compared with Zukoski's (1967) data which were obtained in two-dimensional interaction in a ramp. A good comparison of the present 3-dimensional interaction cases with Zukoski's 2-dimensional interaction case is quite interesting, even though the two class interactions are fundamentally different.

4. Conclusions

An experimental research program establishing data on the surface pressures in swept shock wave/boundary-layer interactions is described. For each of different 32 interaction cases from 4 different freestream Mach numbers, high-spatial-resolution surface pressures are read from several streamwise row of taps connected to a computer-controlled Scanivalve system. These data can serve as a benchmark for a better understanding of shock wave/boundary-layer interactions as well as CFD code validation. Major conclusions from the present experimental study can be summarized as follows:

(1) Utilizing the quasiconical nature of the fin interaction, a simple correlation (first order index) can be posed in terms of p_{peak}/p_∞ vs. M_n only. The weaker the interaction is, the more scatter of the data points (p_{peak}/p_∞) around the correlation curve is observed.

(2) The secondary separation begins to appear near $M_n=1.5$ regardless of freestream Mach number.

(3) The pressure of the secondary peak can be correlated to the normal Mach number and its correlation of the present 3-dimensional interaction cases shows a good comparison with 2-dimensional ramp interaction cases.

(4) The pressure decrease near the fin after the primary attachment line appears in the range of $M_n=1.4\sim1.8$, depending on the freestream Mach numbers.

Acknowledgements

This research was carried out and supported by NASA Grant NAG 2-592. The authors gratefully acknowledge the groundwork of the present research done by Professor Frank Lu.

References

Alvi, F. S. and Settles G. S., 1990, "Structure of Swept Shock Wave/Boundary-Layer Interactions Using Conical Shadowgraphy," *AIAA Paper* 90-1644.

Alvi, F. S. and Settles, G. S., 1991, "Physical Flowfield Model of the Swept Shock/Boundary-Layer Interaction Flowfield, "*AIAA Paper* 91-1768.

Coleman, H. W. and Steel W. G., 1989, *Experimentation and Uncertainty Analysis for Engineers*, John Wile & Sons.

Dolling, D. S., 1993, "Fluctuating Loads in Shock Wave/Turbulent Boundary-Layer Interactions: Tutorial and Update," *AIAA paper* 93-0284.

Garg, S. and Settles, G. S., 1993, "Wall Pressure

Fluctuations Beneath Swept Shock Wave/Boundary Layer Interactions, "*AIAA paper* 93-0384.

Gibson, B. and Dolling, D. S., "Wall Pressure Fluctuations Near Separation in a Mach 5, Sharp Fin-Induced Turbulent Interaction," *AIAA Paper* 91-0646.

Hayes, J. R., 1977, "Prediction Techniques for the Characteristics of Fin Generated Three Dimensional Shock Wave Turbulent Boundary Layer Interactions," AFFDL-TR-77-10.

Kim, K-S., Lee, Y., Alvi, F. S., Settles, G. S. and Horstman, C. C., 1991, "Laser Skin Friction Measurements and CFD Comparison of Weak-to-Strong Swept Shock/Boundary Layer Interactions," *AIAA Journal*, Vol. 29, No. 10, pp. 1643 ~1650.

Knigit, D. and Badekas, D., 1991, "On the Quasi-Conical Flowfield Structure of the Swept Shock Wave-Turbulent Boundary-Layer Interaction," *AIAA Paper* 91-1759.

Lee, Y., Settles, G. S. and Horstmann, C. C., 1994, "Heat Transfer Measurements and Computations of Swept-Shock-Wave/Boundary-Layer Interactions," *AIAA Journal,* Vol. 32, No. 4, pp. 726~734.

Lu, F. K. and Settles, G. S., 1983, "Conical Similarity of Shock/Boundary-Layer Interactions Generated by Swept Fins," *AIAA Paper* 83-756.

Oskam, B., Bogdonoff, S. M. and Vas, I. E., 1975, "Study of Three-Dimensional Flow Fields Generated by the Interaction of a Skewed Shock Wave with a Turbulent Boundary-Layer," AFFDL-TR-75-21, (also see *AIAA Paper* 76-336, 1976).

Settles, G. S. and Dolling, D. S., 1986, "Swept Shock Wave Boundary-Layer Interactions," in *AIAA Progress in Astronautics and Aeronautics: Tactical Missile Aerodynamics,* edited by M. Hemsch and J. Nielsen, Vol. 104, pp. 297-379, AIAA, New York.

Settles, G. S. and Dollign, D. S., 1990, "Swept Shock/Boundary-Layer Interactions-Tutorial and Update," *AIAA paper* 90-0375.

Token, K. H., 1974, "Heat Transfer Due to Shock Wave Turbulent Boundary Layer Interactions on High Speed Weapon System," AFFDL-TR-74-77, Air Force Flight Dynamics Laboratory, WPAFB, Ohio.

Zheltovodov, A. A., Maksimov, A. I. and Shilein, E. K., 1987, "Development of Turbulent Separated Flows in the Vicinity of Swept Shock Waves," edited by Kharitonov, A. M., *Institute of Theoretical and Applied Mechanics; USSR Academy of Sciences,* Novosibrisk, pp. 67~91.

Zubin. M. A. and Ostapenko, N. A., 1979, "Structure of Flow in the Separation Region Resulting from Interaction of a Normal Shock Wave with a Boundary Layer in a Corner," *Izvest. Akad. Nauk S. S. S. R., Mekh. Zhid. i Gaza,* No. 3, 51~58, (English translation).

Zukoski, E. E., 1967, "Turbulent Boundary layer Separation in Front of a Forward Facing Step," *AIAA Journal,* Vol. 5, No. 10, pp. 1746 ~1753.